35th Annual International Conference of the IEEE EMBS
Osaka, Japan, 3 - 7 July, 2013

Superficial Heat Reduction Technique for A Hybrid Microwave-Optical Device

A. Al-Armaghany, K. Tong, and T.S. Leung

Abstract— **Microwave applicator in the form of a circularly polarized microstrip patch antenna is proposed to provide localized deep heating in biological tissue, which causes blood vessels to dilate leading to changes in tissue oxygenation. These changes are monitored by an integrated optical system for studying thermoregulation in different parts of the human body. Using computer simulations, this paper compares circularly and linearly polarized antennas in terms of the efficiency of depositing electromagnetic (EM) energy and the heating patterns. The biological model composes of the skin, fat and muscle layers with appropriate dielectric and thermal properties. The results show that for the same specific absorption rate (SAR) in the muscle, the circularly polarized antenna results in a lower SAR in the skin-fat interface than the linearly polarized antenna. The thermal distribution is also presented based on the biological heat equation. The proposed circularly polarized antenna shows heat reduction in the superficial layers in comparison to the linearly polarized antenna.**

I. Introduction

Elevating the temperature in tissue leads to vasodilation and therefore an increase in blood flow to reduce the excessive heat in the region, a physiological mechanism known as thermoregulation. These thermal responses have been used in various clinical applications to monitor the conditions of the spinal cord injury [1], vascular responses [2] and free flap reconstruction [3]. Currently blood flow measurements such as laser doppler flowmetry (LDF) are restricted to the skin, a rather superficial layer. In conjunction with an electric skin heater, LDF can be used to assess perfusion in the skin [4]. Recently, it has been reported that deep tissue heating in the human calf can be performed using microwave and the corresponding tissue oxygenation changes measured by near-infrared spectroscopy (NIRS) [5]. However, the microwave applicator in this previous study was only able to induce heat in all the layers including the skin, fat and muscle layers. For more localised and selective heating, e.g., muscle heating, it is desirable to minimize the heat in the superficial layers (skin and fat layers) for a more accurate measurement of the oxygenation changes (thermal response) in the muscle layer.

Microwave applicators have been used clinically to induce heat inside tissue for cancer treatments [6] and muscle recovery in sports injuries [7]. The majority of applicators in hyperthermia or diathermy are based on linear polarization for reduced complexity, particularly when operating in near-field region, although circular polarization have been previously reported for reduced stray radiation [8]. Applicators with linear polarization have a fixed electric field component normal to the phantom, whereas with circular polarization (CP) the electric field component rotates in time and through the propagating medium. This approach can reduce superficial heating and increase power deposition in the tissue [9].

This paper focuses on the design of effective microwave applicator and heating pattern in the biological three-layer phantom. The applicator's performance is assessed when it is directly coupled to the tissue. Close proximity can significantly improve the EM energy coupling to the tissue, and also localize the heat distribution [10]. Elevating tissue temperature to 40ºC after 10 minutes exposure is sufficient to monitor the thermal response with NIRS and LDF. We will compare the linear and circular polarizations in terms of SAR and thermal distributions, demonstrating the importance in reducing the skin heating without applying external cooling, e.g., a water bolus.

Fig. 1 shows the hybrid microwave-optical system, consisting of a RF subsystem to generate and amplify 2450 MHz continuous wave (CW) to the applicator. The transmitted and reflected power ratios are monitored to maintain a stable power output and ensure no coupling mismatch during the measurement. The optical monitor was built to measure the changes in oxy and deoxy-haemoglobin concentrations. The optical source consists of six laser diodes operating at six different wavelengths (670, 760, 780, 860, 904, and 980 nm). The light from the six laser diodes is coupled into one optical emitter probe, where the detector probe can measure all six wavelengths. The separation between emitter-detector is set to be 40 mm to ensure desirable light penetration to the muscle. The secondary optical device is based on a commercial LDF monitor with a wavelength of 785 nm, which is used to measure blood flow changed in skin layer. This skin layer result can be used to verify the NIRS measurement of the deeper tissue. A temperature sensor is also integrated with the LDF probe.

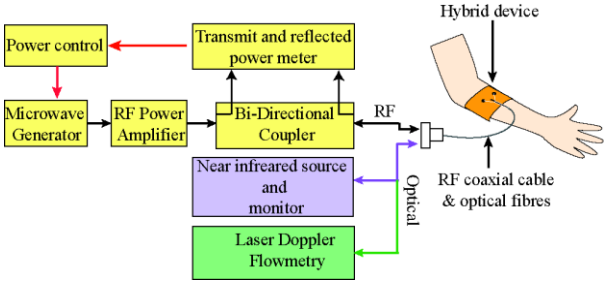

Fig. 1. Hybrid system block diagram

A. Al-Armaghany and K.Tong are with the Department of Electronics and Electrical Engineering, University College London, UK.

T.S. Leung is with the Department of Medical Physics & Bioengineering, University College London, UK.

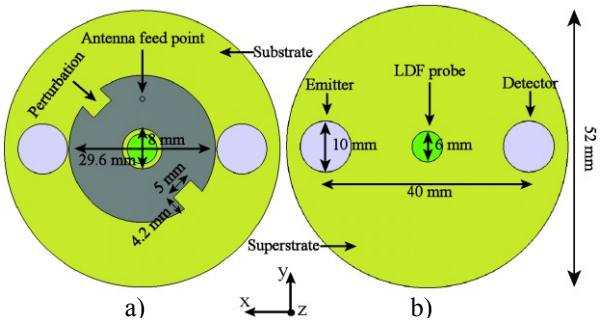

Fig. 2. Applicator geometry, a) annular ring microstrip patch element geometry, b) with superstrate on top.

II. METHODS

Antenna Geometry

As shown in Fig. 2(a), the structure of the applicator is based on a modified annular ring microstrip patch antenna. Conventional linearly polarized annular ring geometry has been previously reported in hyperthermia and other medical applications [11]. The advantages of using an annular ring geometry are compact size and bandwidth enhancement. In our proposed design, the antenna element contains a pair of perturbations in the 45-degree diagonal line of the vertical axis for exciting the TM_{11} mode circular polarization with a single feed point. The specific dimensions of the perturbation splits the two degenerate modes into two orthogonal modes, thus producing CP. The current feed point arrangement produces a left-hand (LH) CP. The diameter of the applicator is 29.6 mm, and the antenna operates at 2450 MHz. The inner slot diameter is 8 mm and the LDF probe is inserted in this central slot. The antenna element is separated from the tissue by a superstrate layer to enhance coupling with an appropriate thickness. The substrate and superstrate are made of higher thermal conductivity material RO6035HTC with a dielectric constant of 3.5. The annular ring geometry enables the NIRS optical emitters and detector to be separated by 40 mm as shown in Fig. 2(b). The overall diameter of the applicator is 52 mm.

III. SIMULATION MODEL

The electromagnetic and thermal simulations have been performed by CST microwave studio 2012 [12]. The phantom model consists of the skin, fat and muscle layers with appropriate electrical properties listed in Table I, and the thermal properties in Table II. The SAR simulation results assume that the absorbed energy is proportional to electrical conductivity of the medium and the deposited electric field. The specific absorption rate in the biological medium is given by:

$$SAR(x,y,z) = \frac{\sigma}{2\rho}\left|E(x,y,z)\right|^2 \quad \text{(W/kg)} \qquad (1)$$

where σ, ρ *and* E are the electrical conductivity (S/m), tissue density (kg/m^3) and deposited electric field (V/m) in the medium, respectively. The SAR can be used to estimate the duration and power requirement for the applicators [13]. Raising the temperature of tissue by 3-4°C would require a SAR of 50 W/kg or greater. However, the SAR equation does not consider the heat production/loss in the tissue due to metabolism and blood flow. Therefore for an accurate thermal simulation, the Penne's bio heat equation is used [14], which solves the temperature distribution of the absorbed energy by taking into account the blood perfusion and metabolic rate. The Pennes bio-heat equation is defined as:

$$\rho c \frac{\partial T}{\partial t} = k\nabla^2 T + \rho(SAR) + Q_m - Q_b\left(T - T_b\right) \qquad (2)$$

$$Q_b = \rho_b c_b W_b \qquad (3)$$

where k is the thermal conductivity and c the heat capacity in the medium. Q_m and Q_b denotes the tissue metabolic heat generation and blood flow coefficient, respectively. T_b is the arterial blood temperature and T is the induced tissue temperature primarily caused by the absorbed EM energy (SAR) in the tissue. ρ_b, c_b and W_b are respectively the density, heat capacity and perfusion rate of the blood.

Fig. 3 shows the simulation setup with the applicator and phantom. The figure also shows the NIRS light path inside tissue covering three layers, which explain why it is essential to solely heat up the muscle, in order to obtain the correct thermoregulation response. As demonstrated in Fig. 3, the LDF probe is only limited to the skin measurement, which is useful for verification of skin heating.

TABLE I
MODELED PHANTOM PARAMETERS

	ε_r	σ (S/m)	ρ (Kg/m^3)	h (mm)
Skin	38	1.46	1100	2
Fat	5.33	0.10	910	10
Muscle	52.86	1.71	1041	60

ε_r = Relative permittivity
h = Modeled tissue thickness.

TABLE II
THERMAL PROPERTIES OF BIOLOGICAL TISSUE

	c (kJ(kg K)$^{-1}$)	k (W(mK)$^{-1}$)	Q_b (Wm^{-3}K^{-1})	Q_m (Wm^{-3})
Skin	3.5	0.293	9100	1620
Fat	2.50	0.201	1700	300
Muscle	3.55	0.53	2700	480

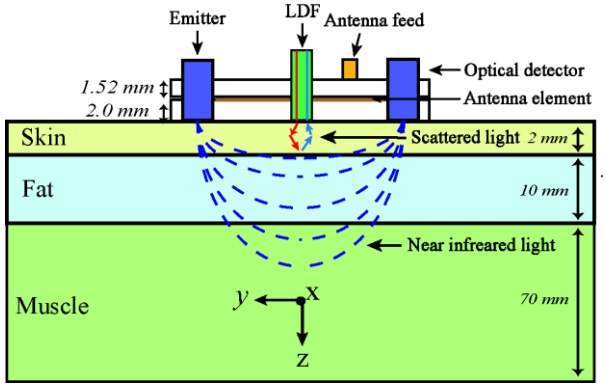

Fig. 3. Phantom model with hybrid devices

IV. Results and Discussion

Simulation results are based on the CP applicator in contrast with the linearly polarized one of the same design excluding the perturbation to maintain a single fundamental mode. The operation of the CP is verified by studying the current distribution on the applicator. Both applicators are optimized to operate at 2450 MHz.

Simulated SAR results are based on the input power of 0.5 W averaged over 1g of tissue. The SAR values are normalized to the peak value for easy comparison. Fig. 4(a) shows the SAR distribution in the yz-plane for linear polarization. The peak SAR of 37.1 W/kg is located around the skin-fat interface in contrast to the local muscle peak SAR of 13.9W/kg, which is about 37% of that in the skin-fat interface. The absorption pattern in the skin is caused by the radiating edges of the antenna at close proximity. The SAR distribution for the CP applicator is shown in Fig. 4(b). It can be seen that the absorbed EM energy in the skin-fat is reduced by 30% with the CP applicator when the muscle SAR is maintained at the same level.

Fig. 5(a) shows the SAR distribution in the xz-plane for the linear polarization. In this plane, there are no radiating edges for linear polarization, therefore the SAR is lower than that in the yz-plane. However, for the CP applicator the EM wave radiates along the perimeter of the annular ring, and this is the reason for a higher SAR in the xz-plane compared to the linear polarized applicator. It is worth mentioning that the peak value remains under 26 W/kg as shown in Fig. 5(b).

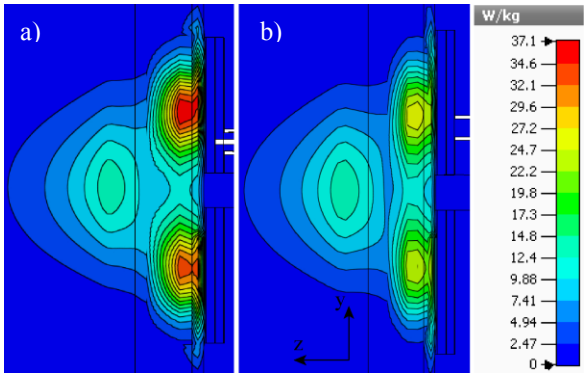

Fig. 4. SAR Distribution across the vertical plane, a) linearly polarized applicator, b) circularly polarized applicator

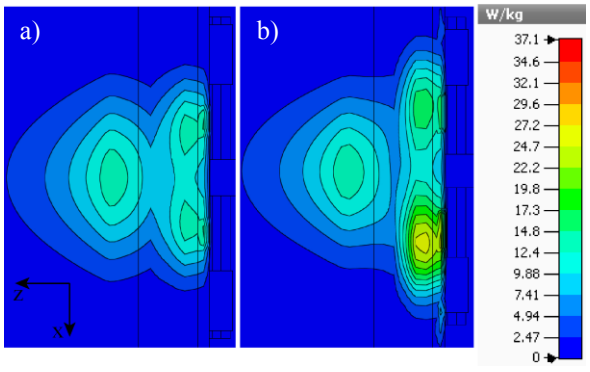

Fig. 5. SAR Distribution across the horizontal plane a) linearly polarized applicator, b) circularly polarized applicator.

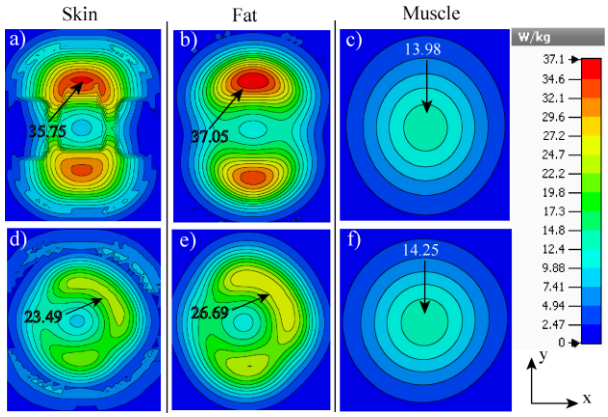

Fig. 6. SAR distribution across different tissue layers, a), b) and c) with linearly polarized applicator, d), e) and f) with circularly polarized applicator

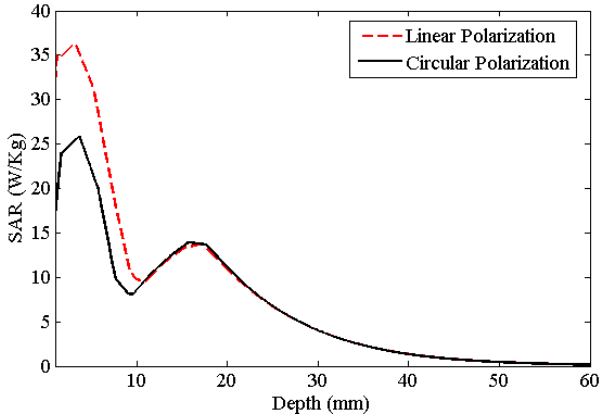

Fig. 7. Peak SAR distribution across all planes

Fig. 6 shows the SAR distributions of each tissue layer across the xy-plane and the peak values. Fig. 6(a) clearly shows the peak SAR on the skin caused by the two radiating edges, a high peak value is located at the upper edge due to the feed point position of the antenna. Fig. 6(b) shows the peak SAR in the fat layer which is 2.7 W/kg higher than that in the skin, and in Fig. 6(c) shows the muscle absorption as all the energy converges into one uniform spot with less than 60% of the peak SAR. Fig. 6(d) shows the SAR in the skin layer across the xy-plane. The absorbed energy is a non-uniform circular distribution as expected by the CP applicator. Higher absorption is noted at the positive y-plane where the feed is located. Fig. 6(e) shows the peak SAR in the fat layer with a similar circular distribution, and in Fig. 6(f) in the SAR forms an uniform spot in the muscle layer.

The peak SAR across all planes is shown in Fig. 7, the results clearly shows that the peak absorption in the skin and fat is reduced by 10 W/kg when using CP applicator. The peak SAR in the muscle is approximately 16 mm below the skin surface with over 50% SAR is achieved.

The transient thermal simulation is performed with the biological heat equation so that the thermal distribution caused by the two types of applicators can be assessed. The simulation duration is based on 10 minute of microwave exposure at a power of 2.5 W RMS for both applicators.

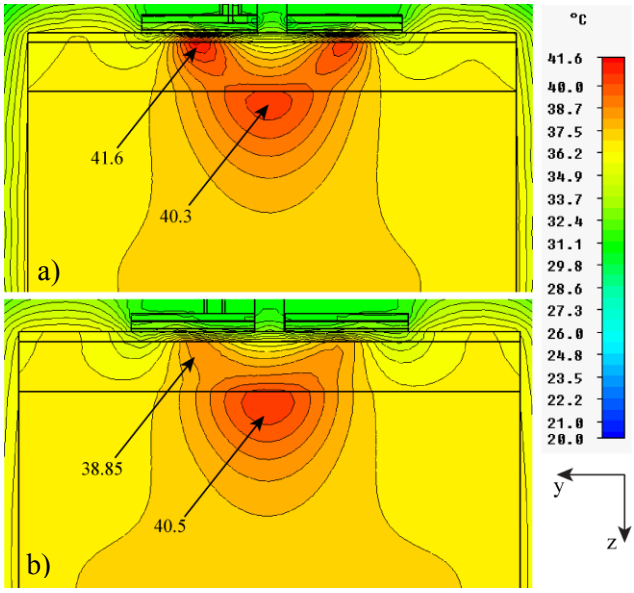

Fig. 8. Simulated thermal distribution of applicators in 10 minutes with (a) linear polarization, (b) circular polarization

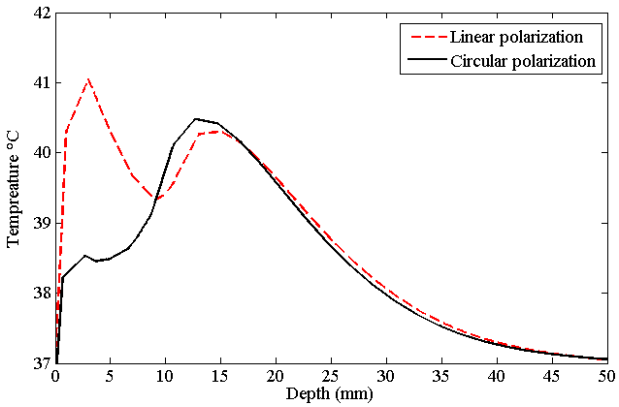

Fig. 9. Peak thermal distribution across all planes

Fig. 8(a) shows the thermal distribution of the linearly polarized applicator in the yz-plane. The peak temperature over 10 minutes of microwave exposure is 41.6 ºC at the skin-fat interface. The peak temperature in the muscle is 40.3 ºC. In contrast to the CP applicator shown in Fig. 8(b), the temperature in the skin-fat interface is reduced by 2.75 ºC, and the peak temperature of 40.5 ºC is in the muscle. Fig. 9 shows the peak thermal distribution across all planes. Again it clearly shows the reduced temperature in the superficial layer with the CP applicator.

V. Conclusion

In this paper we have demonstrated the SAR reduction in the skin-fat interface when using a circularly polarized microstrip patch antenna as the applicator. Moreover we propose a new hybrid applicator and system that induces heat and monitor tissue oxygenation changes in the muscle to provide further information about thermal response.

Results shows that with the circularly polarized antenna the SAR in the muscle is over 50% of the peak absorption, therefore produces efficient heating pattern even without any external cooling. Furthermore, the CP antenna can be further optimized to maintain a uniform circular SAR distribution in the skin and fat layers, which can further improve the efficiency. In the future, we will incorporate external cooling to eliminate the remaining excessive heat in the skin and study the performance of the CP applicator with an anatomical phantom model.

Acknowledgment

This work was partly funded by ESPRC (Grant Code EP/G005036/1).

References

[1] A. Nicotra, M. Asahina, and C. J. Mathias, "Skin vasodilator response to local heating in human chronic spinal cord injury.," *European journal of neurology : the official journal of the European Federation of Neurological Societies*, vol. 11, no. 12, pp. 835–7, Dec. 2004.

[2] G. C. Goats, "Physiotherapy Treatment Modalities Microwave diathermy," *Microwaves*, vol. 24, no. 4, pp. 212–218, 1990.

[3] A. Cornejo, T. Rodriguez, M. Steigelman, S. Stephenson, D. Sahar, S. M. Cohn, J. E. Michalek, and H. T. Wang, "The use of visible light spectroscopy to measure tissue oxygenation in free flap reconstruction.," *Journal of reconstructive microsurgery*, vol. 27, no. 7, pp. 397–402, Oct. 2011.

[4] J. Micheels, B. Aisbjorn, and B. Sorensen, "Laser doppler flowmetry. A new non-invasive measurement of microcirculation in intensive care?," *Resuscitation*, vol. 12, pp. 31–39, 1984.

[5] A. Al-Armaghany, K. Tong, and T. S. Leung., "Development of a Hybrid Microwave-optical Tissue Oxygenation Probe to Measure Thermal Response in the Deep Tissue," *Adv Exp Med Biol*, pp. 1–6, 2012.

[6] P. Wust, B. Hildebrandt, and G. Sreenivasa, "Hyperthermia in combined treatment of cancer," *The lancet oncology*, pp. 487–497, 2002.

[7] A. Giombini, V. Giovannini, A. Di Cesare, P. Pacetti, N. Ichinoseki-Sekine, M. Shiraishi, H. Naito, and N. Maffulli, "Hyperthermia induced by microwave diathermy in the management of muscle and tendon injuries.," *British medical bulletin*, vol. 83, pp. 379–96, Jan. 2007.

[8] C. Chou, A. Guy, and R. Johnson, "SAR in rats exposed in 2,450-□MHz circularly polarized waveguides," *Bioelectromagnetics*, vol. 398, pp. 389–398, 1984.

[9] R. L. Magin and a F. Peterson, "Noninvasive microwave phased arrays for local hyperthermia: a review.," *International journal of hyperthermia : the official journal of European Society for Hyperthermic Oncology, North American Hyperthermia Group*, vol. 5, no. 4, pp. 429–50, 1989.

[10] A. Guy, "Electromagnetic fields and relative heating patterns due to a rectangular aperture source in direct contact with bilayered biological tissue," *... Theory and Techniques, IEEE Transactions on*, 1971.

[11] I. Bahl, S. Stuchly, and M. Stuchly, "A new microstrip radiator for medical applications," *Microwave Theory and ...*, pp. 1464–1468, 1980.

[12] "Computer Simulation Technology Microwave Studio," *http://www.cst.com*, 2012. .

[13] A. Vander Vorst, A. Rosen, and Y. Kotsuka, *RF/Microwave Interaction with Biological Tissues (Wiley Series in Microwave and Optical Engineering)*. Wiley-Blackwell, 2006, pp. 344, 288–291,12–14.

[14] H. H. Pennes, "Analysis of tissue and arterial blood temperatures in the resting human forearm.," *Journal of Applied Physiology*, vol. 1, no. 2, pp. 93–122, 1948.